

Cooperative behavior of Zn cations in Bi-based perovskites: A comparison of $(\text{Bi,Sr})_2\text{ZnNbO}_6$ and $(\text{Bi,Sr})_2\text{MgNbO}_6$

Shigeyuki Takagi,^{1,2} Valentino R. Cooper,¹ and David J. Singh^{1,*}¹*Materials Science and Technology Division, Oak Ridge National Laboratory, Oak Ridge, Tennessee 37831-6114, USA*²*Department of Physics, University of Tennessee, Knoxville, Tennessee 37996, USA*

(Received 20 January 2011; revised manuscript received 15 February 2011; published 21 March 2011)

We investigated the polar behavior of the double perovskite $(\text{Bi,Sr})_2\text{MgNbO}_6$ using first-principles density-functional theory calculations. We find that the magnitude ($75 \mu\text{C}/\text{cm}^2$) and direction (along [111]) of the polarization are comparable to our previous results for the *A*-site size difference $(\text{Bi,Sr})_2\text{ZnNbO}_6$ and $(\text{Bi,Pb})_2\text{ZnNbO}_6$ systems. However, comparisons with the $(\text{Bi,Sr})_2\text{ZnNbO}_6$ compound indicate that the presence of Zn modestly enhances the off-centering of the Sr and Nb cations as well as the Born effective charges of both Bi and Nb. Analogous to the corresponding Pb-based perovskites, $\text{Pb}(\text{Mg}_{1/3}\text{Nb}_{2/3})\text{O}_3$ and $\text{Pb}(\text{Zn}_{1/3}\text{Nb}_{2/3})\text{O}_3$, we demonstrate that the differences in the experimentally observed critical temperatures are related to the differences in polarization between the two materials. A local dipole analysis indicates that the most significant contribution arises from the enhanced cooperative couplings with the larger Zn displacements.

DOI: [10.1103/PhysRevB.83.115130](https://doi.org/10.1103/PhysRevB.83.115130)

PACS number(s): 77.84.Ek, 71.20.Ps

I. INTRODUCTION

Perovskite oxides have been studied extensively for many years because of their variety of properties, which are not only of technological importance but of scientific interest. While the ideal ABO_3 structure has cubic symmetry, *A*-O and *B*-O interactions can easily result in distortions that produce a spontaneous polarization.^{1,2} In general, large piezoelectric responses occur near morphotropic phase boundaries where the polarization can rotate between the rhombohedral and the tetragonal directions.^{3–8} Many current research efforts have been focused on improving the electromechanical responses in these materials through alloying. For example, the addition of PbTiO_3 (PT) to the relaxors $\text{Pb}(\text{Mg}_{1/3}\text{Nb}_{2/3})\text{O}_3$ (PMN) and $\text{Pb}(\text{Zn}_{1/3}\text{Nb}_{2/3})\text{O}_3$ (PZN) gives rise to an ultrahigh piezoelectric response, which is 10 times higher than that of the most commonly used piezoelectric ceramic PbZrO_3 - PbTiO_3 (PZT).^{3,9}

Understanding the interplay between chemistry and patterns of lattice instabilities, in particular, those related to ferroelectric and tilt modes, is crucial for progress. In this paper, we examine the nature of the *B*-site, Zn and Mg, cations within BSMN and BSZN. Mg^{2+} and Zn^{2+} have approximately the same ionic size ($r_{\text{Mg}^{2+}} = 0.86 \text{ \AA}$ and $r_{\text{Zn}^{2+}} = 0.88 \text{ \AA}$),¹⁶ but unlike Zn, Mg has no occupied *d* states. In both BSMN and BSZN, strong ferroelectricity is expected due to the large *A*-site size difference between Bi and Sr, the presence of stereochemically active Bi^{3+} ions, which enhance ferroelectric instabilities, and high-Born charge Nb^{5+} cations, which also favor ferroelectricity as in KNbO_3 . We find that the larger off-centering of the Zn cations relative to Mg correlates with the higher T_c observed within the Zn materials. This means that the behavior of Zn in these materials is similar to what is observed in Pb-based compounds.

Related to this, a first-principles study, using ordered supercells, concluded that the larger piezoelectric coefficient, e_{33} , of 0.60PMN-0.40PT relative to that of PZT is derived from the large cooperative displacements of Pb, Ti, Nb, and O atoms.¹⁰ In PZN-PT, the displacements of Pb, Ti, and Nb ions

were shown to be further enhanced by the larger off-centering of Zn ions as opposed to the Mg ions in PMN-PT.¹¹ Here there is a simple quadratic relationship between the temperature at the dielectric constant maximum, $T_{\epsilon,\text{max}}$, and the local polarization (which arises from cation off-centering) within this class of Pb-based ferroelectrics, thereby emphasizing the role that the off-centering of Zn cations plays in defining transition temperatures observed in these materials. Thus, it is indispensable to understand how atomic character affects the macroscopic properties in order to establish a rational procedure for tuning the pertinent properties of these materials through compositional modification.

We present a density-functional theory (DFT) study of the polar behavior of the double perovskite $(\text{Bi,Sr})_2\text{MgNbO}_6$ (BSMN) and compare these results with those of our former investigation for $(\text{Bi,Sr})_2\text{ZnNbO}_6$ (BSZN).¹² The goal of this work is to understand the role that *B*-site cations play in the ferroelectricity of Bi-based perovskites with a large *A*-site size difference. In a recent DFT calculation, it was demonstrated that the presence of *A*-site cations with different ionic radii promotes ferroelectricity through increased *A*-site off-centering.¹³ In this case, the underlying mechanism relies on suppression of the BO_6 octahedral tilting that inherently counters ferroelectric modes in a material. In this vein, we reported on the polar behavior of the double perovskites, $(\text{Bi,Pb})_2\text{ZnNbO}_6$ and $(\text{Bi,Sr})_2\text{ZnNbO}_6$. The large ionic size difference on the *A*-site was found to contribute to the large polarization values of $\sim 80 \mu\text{C}/\text{cm}^2$,¹² which are comparable to those of BiFeO_3 ($90\text{--}100 \mu\text{C}/\text{cm}^2$).¹⁴ Subsequently, in the $(\text{Bi,Na})_2\text{ScNbO}_6$, $(\text{Bi,K})_2\text{ScNbO}_6$, and $(\text{Bi,Rb})_2\text{ScNbO}_6$ series of compounds, we showed that a larger *A*-site size difference leads to enhanced off-centering of Bi and Nb ions.¹⁵ In all cases, the polarization was due to a combination of the large off-centering of Bi ions, which have stereochemical activity and much lower ionic radii relative to other *A*-site ions, and the cooperative (although much lower in magnitude) off-centering of Nb ions that have highly enhanced Born effective charges.

Indeed, we find that both BSMN and BSZN structures have high polarizations: 75 and 79 $\mu\text{C}/\text{cm}^2$, respectively. Applying the quadratic relationship between \vec{P} and $T_{\epsilon,\text{max}}$, previously derived for Pb-based perovskite ferroelectrics,¹¹ we demonstrate that the difference in \vec{P} is responsible for the 120 K difference in the experimental phase transition temperatures of the two structures. (Note: BSMN and BSZN were previously experimentally determined to be ferroelectric, with the relatively high phase transition temperatures of 803 and 923 K, respectively.^{17,18}) Using an analysis of the contribution of the local dipole moment interactions to the transition temperature, we show that it is the coupling between Zn^{2+} and other cations that promotes the higher transition temperature of the BSZN compound, thus emphasizing the cooperative nature of Zn off-centering within these materials. Hence, Zn plays a similar role in these Bi-based materials as in Pb-based piezoelectrics.

II. APPROACH

The double perovskite $(\text{Bi,Sr})_2\text{MgNbO}_6$ was studied using DFT within the local-density approximation (LDA). This approximation, similar to other density functionals such as the generalized gradient approximation (GGA) of Perdew and co-workers,¹⁹ is known to underestimate band gaps. However, it has been widely used to calculate structural properties and polarizations in ferroelectrics, where results in very good agreement with experiment are obtained, while standard GGA functionals have been shown to severely overestimate the ferroelectric instabilities, giving much higher c/a ratios and bond lengths than experiment.²⁰

All calculations, including polarizations and Born effective charges, were performed using a plane-wave basis and ultrasoft pseudopotentials²¹ as implemented in the Quantum Espresso package.²² All results were converged with respect to the cutoff energy (30 eV) and Brillouin zone sampling (Monkhorst-Pack $4 \times 4 \times 4$ k -point mesh), as in our previous studies.^{12,15}

Due to the large differences in both charge state and ionic size between Mg^{2+} and Nb^{5+} , we assumed B -site double-perovskite ordering. This is consistent with what is seen in the relaxor compound PMN, where a 1:1 ordering takes place even though it has a 1:2 stoichiometry.^{23–26} The 1:1 B -site stoichiometry of the current material should promote this ordering. Although there is no *a priori* reasoning for determining the A -site ordering, an ordered double-perovskite A site was also used. This was done to avoid including an extrinsic polarization arising from the particular polar space group and for direct comparisons with previous BSZN results which employed a similarly ordered supercell.¹² (See Fig. 1.)

While the large A -site size difference in this material favors large A -site off-centering, BO_6 octahedral tilt modes which compete with the ferroelectric instabilities are also expected. Therefore, it is necessary that the supercell has an even number of units along the [001], [010], and [100] directions to accommodate the various Glazer tilt patterns.²⁷ Hence, we simulated a 40-atom $2 \times 2 \times 2$ supercell. Similar 40-atom cells were determined to be sufficient for extracting the tilt patterns in the PZT solid solution and should give us a reasonable understanding of the differences in Zn and Mg chemistries in Bi-based materials.²⁸

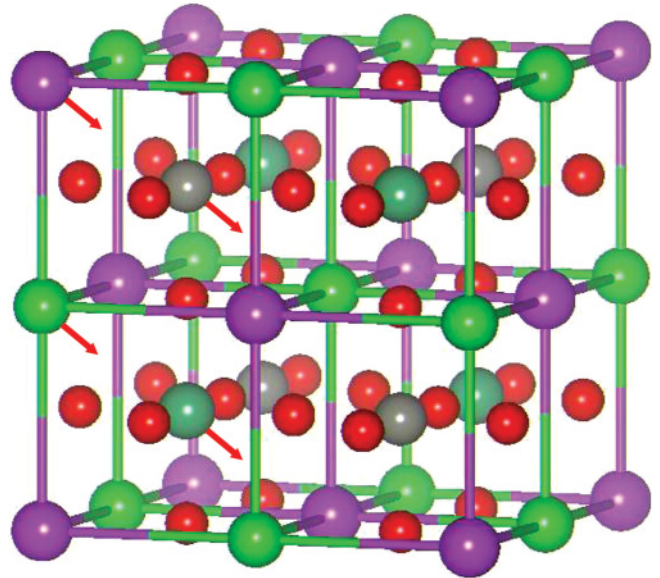


FIG. 1. (Color online) Schematic of the ordered double-perovskite structure. Bi, Sr, Zn/Mg, Nb, and O ions are denoted by light purple, light green, dark green, gray, and red spheres, respectively. Cation off-centering directions are denoted by (red) arrows.

III. ATOMIC AND ELECTRONIC STRUCTURE

For the pseudocubic BSMN structure we optimized the lattice parameters, by first relaxing all atomic coordinates without any symmetry operations and then evaluating the energetics as a function of the lattice parameter to find the equilibrium volume. The calculated LDA lattice parameter of 3.97 Å was found to be in good agreement with the room-temperature experimental value of 4.001 Å.¹⁸ The small difference of $\sim 1\%$ with respect to the experimental value is typical of LDA calculations of oxide ferroelectrics and is a result of the LDA volume errors. We confirmed that our results are robust against the LDA volume error, as identical displacement patterns were obtained at the experimental volume.

Figure 2 shows the cation off-centerings along the Cartesian directions and their magnitudes with respect to the center of their O cages in a relaxed 40-atom pseudocubic BSMN supercell. Importantly, all cations off-center along a [111] direction, indicating a strong preference for this ferroelectric direction. Also, we calculated the energetics as a function of imposed tetragonal strain at the equilibrium volume. The lowest energy structure was found to have a $c/a = 1.000$, corresponding to x-ray phase analysis results, where inappreciable distortions were observed.¹⁸ Over the range considered ($0.94 < c/a < 1.06$), all cation off-centering remained essentially along the [111] direction, implying strong stability of the rhombohedral ferroelectric state.

The off-center displacements of the Mg cations can be fully understood from a bond-valence perspective.²⁹ In an ideal perovskite structure, Mg ions would be overbonded (i.e. their bond-valence sum would yield a charge greater than their nominal charge of +2).^{30,31} Typically, this sum can be reduced through the accommodation of off-center displacements along

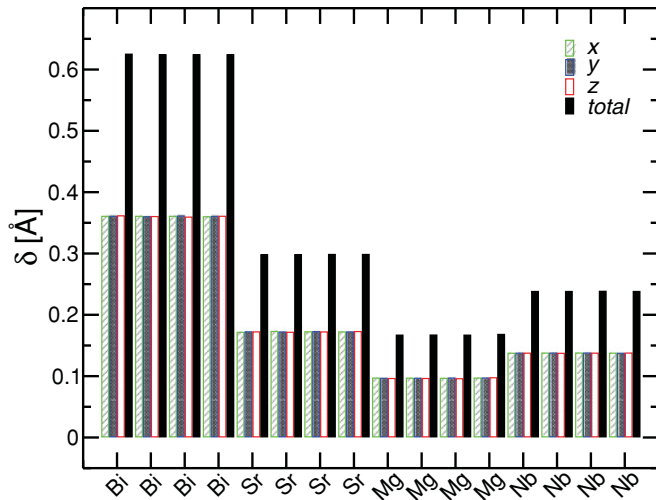


FIG. 2. (Color online) Magnitude and direction of cation off-centering relative to the center of their O cages (i.e., 12 nearest O ions for the *A* site and 6 nearest O ions for the *B* site) along the Cartesian directions for a relaxed 40-atom BSMN supercell. Note: All cations off-center along a [111] direction, and the magnitudes of off-centering are roughly equal for a given cation type.

[111], which are coupled to two types of structural distortions: (i) an increase in octahedral volume and (2) the introduction of octahedral tilts. In this case we find that the Mg octahedra volume of 11.71 \AA^3 is larger than the Nb volume (10.27 \AA^3). Similarly, we find octahedral rotations and tilts of the order of 8° and 7° , respectively. The combination of this larger volume and octahedral distortions favors the displacement of Mg cations along [111] within the unit cell.

Figure 3 depicts the total and projected electronic density of states of the relaxed pseudocubic BSMN supercell. The valence band is comprised mainly of O *2p* states, while the conduction band is mostly of an unoccupied metal character. The calculated LDA band gap was 3.1 eV. This may be

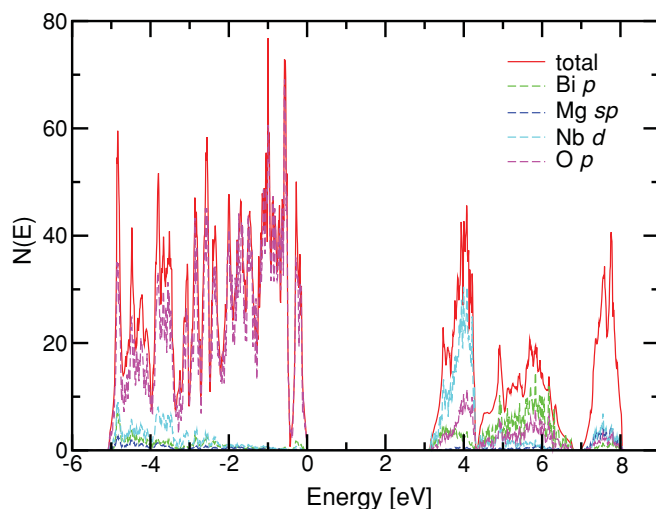


FIG. 3. (Color online) Total electronic density of states and projections onto Bi *p*, Mg *sp*, Nb *d*, and O *p* states for a relaxed pseudocubic BSMN supercell. The valence band maximum is set to 0.

TABLE I. Structural and electronic properties of BSMN and BSZN. *a*, Z^* , δ , and *P* denote the equilibrium pseudocubic lattice parameter, average Born effective charge, average magnitude of cation off-centering with respect to O cages, and magnitude of polarization (which points mainly along the [111] direction), respectively.

	(Bi,Sr) ₂ MgNbO ₆	(Bi,Sr) ₂ ZnNbO ₆
<i>a</i> (LDA)	3.97 Å	3.97 Å
<i>Bi</i>		
δ	0.62 Å	0.62 Å
Z^*	4.3	4.4
<i>Sr</i>		
δ	0.30 Å	0.33 Å
Z^*	2.6	2.6
<i>Mg/Zn</i>		
δ	0.17 Å	0.25 Å
Z^*	2.6	2.8
<i>Nb</i>		
δ	0.24 Å	0.25 Å
Z^*	5.6	5.8
<i>P</i>	75 $\mu\text{C}/\text{cm}^2$	79 $\mu\text{C}/\text{cm}^2$

underestimated due to the LDA band-gap error. Thus, the material is expected to be a good insulator at ambient temperature. The computed polarization for the supercell using the Berry phase method is $75 \mu\text{C}/\text{cm}^2$. For comparison, the computed polarization of BSZN is $79 \mu\text{C}/\text{cm}^2$.¹² The average Born effective charges are Bi = 4.3, Sr = 2.6, Mg = 2.6, and Nb = 5.6. These values are enhanced relative to their nominal charges and reflect the effects of hybridization with O *2p* states.

IV. DISCUSSION

To examine the role of the *B*-site Zn ion in Bi-based perovskites with a large *A*-site size difference, we examine and compare our previously obtained results for BSZN.¹² Table I lists the average cation off-centering δ and the Born effective charges for BSMN and BSZN. Although both compounds have the same equilibrium volume, the Zn-containing material has a larger polarization, $79 \mu\text{C}/\text{cm}^2$, compared to a polarization of $75 \mu\text{C}/\text{cm}^2$ in BSMN. Inspection of the average *B*-site cation displacements shows that Zn ions off-center $\sim 32\%$ more than Mg ions (even though the ionic radius of Zn is slightly larger than that of Mg). Furthermore, there is a modest increase in the average off-center displacements of Sr ions on the *A* site in BSZN. The larger off-centering of Zn ions relative to Mg ions fosters slightly greater Sr and Nb off-center displacements (see Fig. 1), thus emphasizing the cooperative nature of the cation displacements. From a bond-valence perspective, this off-centering is expected, as the larger off-centering of Zn results in overbonding of the O cations that Zn moves toward and underbonding of the cations it moves away from, thus to counter this effect, other cations would be expected to off-center. Interestingly, however, no difference in Bi off-centering is observed. From a structural point of view, we see very few changes in the Zn octahedral volume (11.85 \AA^3), octahedral rotations (9°) and tilts (7°) compared to Mg. This suggests that there is a fundamental

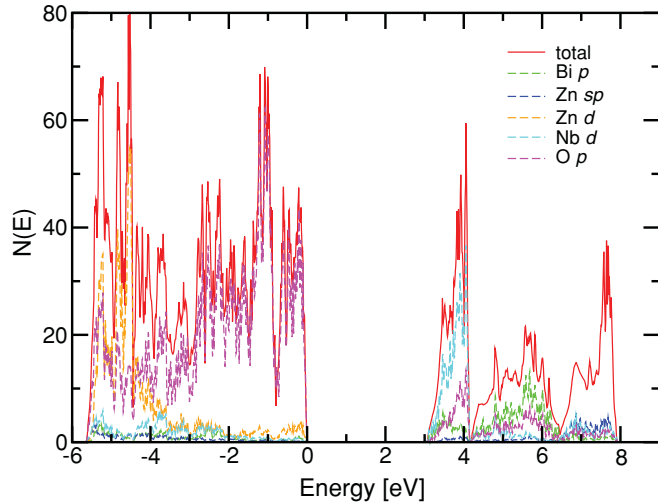


FIG. 4. (Color online) Total electronic density of states and projections onto Bi p , Zn sp , Nb d , and O p states for a relaxed pseudocubic BSZN supercell. The valence band maximum is set to 0.

difference in the electronic structure that contributes to the significant increase in Zn displacement.

Figure 4 depicts the total and projected electronic density of states of the pseudocubic relaxed BSZN supercell, showing features similar to those of BSMN. As expected, the primary difference is the presence of occupied Zn d states at the bottom of the valence band that strongly hybridize with O $2p$ bands. More significantly, this hybridization weakens the short-range repulsions which stabilize the cubic phase, promoting the off-centering of Zn ions relative to Mg ions. In addition, we find slightly higher Bi, Zn and Nb Born effective charges in the Zn containing compound. Ultimately, it is the combination of the larger cooperative cation off-centering and the higher Born effective charges which contribute to the increase in BSZN polarization.

To elucidate the Zn contribution to higher polarizations, we examine a hypothetical BSMN structure constructed from equilibrium pseudocubic atomic coordinates of BSZN (i.e., in the BSZN relaxed structure all Zn ions are replaced with Mg). The Born effective charges and polarization calculated with the equilibrium BSZN structure are listed in Table II. Despite the artificially larger off-center displacement of Mg in this structure, there is no increase in the Born effective charges of Bi, Sr, Mg, or Nb. In addition, the polarization for BSMN is still lower than that for BSZN, possibly reflecting the more covalent character of Zn-O interactions, which enhance the Born effective charges and off-center displacements of Zn cations. In other words, it is the more covalent Zn-O interactions which seem to drive the larger polarization within Zn-containing compounds. Similar covalent-like interactions were also observed in the $\text{Bi}_2\text{MgTiO}_6$ and $\text{Bi}_2\text{ZnTiO}_6$ systems.³² This can be viewed as a second-order Jahn-Teller effect involving Zn, which is related to the first-order effect involving Cu^{2+} in fluorite-type crystals, but with a closed d shell.³³

We explore the cooperative nature of Zn cation off-centering by examining the relationship between $T_{\epsilon, \max}$ and \vec{P} . Previously, Grinberg and Rappe proposed that for a wide

TABLE II. Comparison of Born effective charges and polarizations for BSMN and BSZN calculated with the equilibrium pseudocubic structure of BSZN, where Z^* denotes the average Born effective charge and $P(111)$ is the magnitude of polarization along the $[111]$ direction, respectively.

	$(\text{Bi,Sr})_2\text{MgNbO}_6$	$(\text{Bi,Sr})_2\text{ZnNbO}_6$
Z^*		
Bi	4.3	4.4
Sr	2.6	2.6
Mg/Zn	2.6	2.8
Nb	5.5	5.8
$P(111)$	$76 \mu\text{C}/\text{cm}^2$	$79 \mu\text{C}/\text{cm}^2$

range of Pb-based perovskite ferroelectrics,

$$T_{\epsilon, \max} = \gamma \left(\sum_i \frac{P_{0i}}{N} \right)^2 = \gamma \left(\sum_i \frac{Z_i^* \cdot \mathbf{u}_i}{NV_0} \right)^2, \quad (1)$$

where γ is a constant determined from fitting of a large dataset of Pb-based perovskite ferroelectrics, and P_{0i} is the local dipole moment/unit volume (V_0) for N primitive cells of the i th cation as defined by its Born effective charge Z_i^* and the off-center displacement \mathbf{u}_i . Table III lists the T_c values determined from Eq. (1). Using the predetermined Grinberg and Rappe γ we compute values of 641 and 533 K for BSZN and BSMN, respectively. It should be noted that this γ was determined for Pb-based perovskite and therefore it may be constructive to redefine this value for Bi-based perovskites. Nevertheless, we find that the difference in T_c (108 K) is in good agreement with experiment (120 K). The origin of this difference can be further analyzed by expanding Eq. (1) in terms of local dipole-dipole interactions as

$$T_{\epsilon, \max} = \gamma \sum_i \sum_j \frac{P_{0i} \cdot P_{0j}}{N}. \quad (2)$$

Table III lists the the local dipole contributions to the transition temperature for BSMN and BSZN. It can be clearly seen that in both materials the dominant contributions to $T_{\epsilon, \max}$ arise from interactions involving Bi and Nb. This

TABLE III. Local dipole contribution to $T_{\epsilon, \max}$ (in K) for BSMN and BSZN as computed from Eq. (2) with $\gamma = 1189$. Δ is the difference between BSZN and BSMN.

	$(\text{Bi,Sr})_2\text{MgNbO}_6$	$(\text{Bi,Sr})_2\text{ZnNbO}_6$	Δ
Bi·Bi	139	145	7
Sr·Sr	12	14	2
Zn/Mg·Zn/Mg	4	10	6
Nb·Nb	35	41	6
Bi·Sr	81	91	10
Bi·Zn/Mg	46	74	29
Bi·Nb	140	154	15
Sr·Zn/Mg	13	23	10
Sr·Nb	41	48	8
Zn/Mg·Nb	23	40	16
Total	533	641	108

emphasizes the importance of the large off-centering of Bi and Born effective charges of the Nb cations within these materials. However, we also find that the large differences in $T_{\epsilon, \max}$ arise mainly from couplings of the strongly polar Bi and Nb cations with the Zn cation. This, once again, enforces the idea that cooperative interactions, specifically, dipole-dipole interactions with Zn cations, favor enhanced transition temperatures as well as polarizations within these materials.

V. CONCLUSIONS

In summary, we have performed DFT calculations to compare and contrast the polar behavior of the double perovskites $(\text{Bi,Sr})_2\text{MgNbO}_6$ and $(\text{Bi,Sr})_2\text{ZnNbO}_6$. Both materials have high polarizations along the [111] direction, however, the polarization in BSMN is slightly lower than that in $(\text{Bi,Sr})_2\text{ZnNbO}_6$. In the latter case, we find that the presence of Zn ions induce much larger cooperative displacements of the metal cations. Here, the Zn 3d states strongly hybridize with the O 2p states, thereby leading to enhanced Born effective charges relative to Mg. In any event, the more covalent-like interactions between Zn-O (as exemplified in the higher Zn

effective charge) increase the off-centering of Zn ions and promote a modest increase in the off-centering of Sr ions. Once again, we note that similar covalent-like interactions were also observed in the $\text{Bi}_2\text{MgTiO}_6$ and $\text{Bi}_2\text{ZnTiO}_6$ systems.³² Simultaneously, we observe that the Zn containing material also has enhanced Born effective charges of Bi and Nb ions relative to the Mg compound. The combination of larger cooperative cation displacements and Born effective charges in Zn-containing compounds is manifested as an increase in both the polarization and the transition temperature of BSZN. The smaller off-centering of Mg ions observed here was previously seen in PMN³⁴ and PMN-PT¹⁰ and demonstrates that the behavior of Zn and Mg cations in the A-site size difference, Bi-based compounds is indeed analogous to that found in Pb-based perovskites such as PMN, PZN, PZN-PT, and PMN-PT and may be general for all ferroelectric perovskites.

ACKNOWLEDGMENTS

This work was supported by the Division of Materials Sciences and Engineering, Office of Basic Energy Sciences, US Department of Energy (V.R.C., D.J.S.) and the Office of Naval Research (S.T., D.J.S.).

*singhdj@ornl.gov

¹R. E. Cohen and H. Krakauer, *Phys. Rev. B* **42**, 6416 (1990).

²R. E. Cohen, *Nature* **358**, 136 (1992).

³S.-E. Park and T. R. ShROUT, *J. Appl. Phys.* **82**, 1804 (1997).

⁴B. Noheda, D. E. Cox, G. Shirane, L. E. Cross, and Z. Zhong, *Appl. Phys. Lett.* **74**, 2059 (1999).

⁵L. Bellaiche, A. Garcia, and D. Vanderbilt, *Phys. Rev. Lett.* **84**, 5427 (2000).

⁶H. Fu and R. E. Cohen, *Nature* **403**, 281 (2000).

⁷R. Guo, L. E. Cross, S.-E. Park, B. Noheda, D. E. Cox, and G. Shirane, *Phys. Rev. Lett.* **84**, 5423 (2000).

⁸B. Noheda, D. E. Cox, G. Shirane, S.-E. Park, L. E. Cross, and Z. Zhong, *Phys. Rev. Lett.* **86**, 3891 (2001).

⁹R. E. Service, *Science* **275**, 1878 (1997).

¹⁰L. Bellaiche and D. Vanderbilt, *Phys. Rev. Lett.* **83**, 1347 (1999).

¹¹I. Grinberg and A. M. Rappe, *Phys. Rev. B* **70**, 220101(R) (2004).

¹²S. Takagi, A. Subedi, D. J. Singh, and V. R. Cooper, *Phys. Rev. B* **81**, 134106 (2010).

¹³D. J. Singh and C. H. Park, *Phys. Rev. Lett.* **100**, 087601 (2008).

¹⁴J. B. Neaton, C. Ederer, U. V. Waghmare, N. A. Spaldin, and K. M. Rabe, *Phys. Rev. B* **71**, 014113 (2005).

¹⁵S. Takagi, A. Subedi, V. R. Cooper, and D. J. Singh, *Phys. Rev. B* **82**, 134108 (2010).

¹⁶R. D. Shannon, *Acta Crystallogr. Sect. A* **32**, 751 (1976).

¹⁷D. D. Khalyavin, A. N. Salak, N. P. Vyshatko, A. B. Lopes, N. M. Olekhovich, A. V. Pushkarev, I. I. Maroz, and Y. V. Radyush, *Chem. Mater.* **18**, 5104 (2006).

¹⁸L. G. Kosyachenko, V. V. Kochetkov, A. G. Belous, V. V. Bogatko, and Yu. N. Venevtsev, *Izv. Akad. Nauk SSSR Neorg. Mater.* **18**, 1352 (1982).

¹⁹J. P. Perdew, K. Burke, and M. Ernzerhof, *Phys. Rev. Lett.* **77**, 3865 (1996).

²⁰Z. Wu, R. E. Cohen, and D. J. Singh, *Phys. Rev. B* **70**, 104112 (2004).

²¹D. Vanderbilt, *Phys. Rev. B* **41**, 7892 (1990).

²²P. Giannozzi *et al.*, *J. Phys. Condens. Matter* **21**, 395502 (2009).

²³A. D. Hilton, D. J. Barber, C. A. Randall, and T. R. ShROUT, *J. Mater. Sci.* **25**, 3461 (1990).

²⁴H. B. Krause and D. L. Gibbon, *Z. Kristallogr.* **134**, 44 (1971).

²⁵P. K. Davies and M. A. Akbas, *J. Phys. Chem. Solids* **61**, 159 (2000).

²⁶S. A. Prosandeev, E. Cockayne, B. P. Burton, S. Kamba, J. Petzelt, Y. Yuzyuk, R. S. Katiyar, and S. B. Vakhrushev, *Phys. Rev. B* **70**, 134110 (2004).

²⁷A. M. Glazer, *Acta Crystallogr. Sect. B* **28**, 3384 (1972).

²⁸I. Grinberg, V. R. Cooper, and A. M. Rappe, *Nature* **419**, 909 (2002).

²⁹I. D. Brown, *Structure and Bonding in Crystals II* (Academic, New York, 1981), pp. 1–30.

³⁰I. Grinberg, V. R. Cooper, and A. M. Rappe, *Phys. Rev. B* **69**, 144118 (2004).

³¹V. R. Cooper, I. Grinberg, and A. M. Rappe, *AIP Conf. Proc.* **677**, 220 (2003).

³²H. Wang, H. Huang, W. Lu, H. L. W. Chan, B. Wang, and C. H. Woo, *J. Appl. Phys.* **105**, 053713 (2009).

³³P. García Fernández, J. A. Aramburu, M. T. Barriuso, and M. Moreno, *Phys. Rev. B* **69**, 174110 (2004).

³⁴M. Suewattana and D. J. Singh, *Phys. Rev. B* **73**, 224105 (2006).